ChemComm

FEATURE ARTICLE

View Article Online
View Journal | View Issue



Cite this: *Chem. Commun.*, 2025, **61**, 1761

# Advances in lanthanide cyclononatetraenyl chemistry

Xiaofei Sun, *[a] Grégory Nocton [b] and Peter W. Roesky *[ac]

Received 4th November 2024,
Accepted 5th December 2024

DOI: 10.1039/d4cc05896h

rsc.li/chemcomm

Cyclononatetraenyl (Cnt) is a nine-membered monoanionic aromatic ligand. Despite its early discovery in 1963, it has been rarely utilised in coordination chemistry, which is mainly due to its large diameter and easy skeletal rearrangement. Only in 2017, the first lanthanide Cnt complex was synthesised, marking the beginning of a new era in organolanthanide chemistry. Since then, the chemistry displayed by Cnt has expanded rapidly in lanthanide chemistry. Due to the ligand flexibility, both classical planar $\eta^9$-Cnt ligands and heavily bent ones with lower hapticity were found in Ln coordination complexes. These novel structure motifs exhibit reactivity which differs significantly from traditional cyclopentadienyl (Cp) and cyclooctatetraenediide (Cot) complexes. Some of the obtained compounds also show interesting photoluminescence and magnetic properties. This review presents an overview of the synthesis, structure and reactivity of the growing family of lanthanide Cnt compounds.



## Introduction

Since Faraday isolated benzene in 1825,[1] aromaticity has become a fundamental concept in chemistry. Although defining aromaticity can be challenging today, with various criteria and definitions being developed,[2] the classical way to define aromatic compounds relies on Hückel's $(4n + 2)\pi$ electron rule.[3] In general, aromatic C-based monocyclic ring systems are frequently used as ligands in coordination chemistry (Fig. 1). The discovery of the first metallocene (ferrocene) in 1951 by Kealy and Pauson,[4] and its subsequent structural elucidation[5] was a milestone in modern chemistry. In ferrocene, the iron centre is sandwiched between two aromatic monoanionic cyclopentadienyl (Cp) ligands. Shortly after the discovery of ferrocene, the Cp ligand was also introduced in organolanthanide chemistry. In 1954, Wilkinson and Birmingham reported the first organolanthanide compounds, namely, the tris(cyclopentadienyl)lanthanides $[(Cp)_3Ln^{III}]$.[6] Since then, Cp-type ligands have played a dominating role in lanthanide chemistry.

Following the widespread use of Cp ligands, the 10π-aromatic cyclooctatetraenediide (Cot) dianion has also played a crucial role in the chemistry of f-elements for more than five decades.[7,8] Lanthanide complexes featuring Cp or Cot ligands have become important not only due to their unique structures but also their potential applications in catalysis, electrochemistry, and material science. Beyond the ubiquitous Cp and Cot rings in organolanthanide chemistry, other aromatic carbocycles have also been employed as ligands. A significant step was made by Cloke *et al.* in 1987 when they synthesized several lanthanide bis(arene) sandwich compounds with bulky benzene derivatives using electron-beam vaporization techniques.[9] Very recently, the first examples of lanthanide complexes comprising the four-membered substituted cyclobutadienyl dianion have also been disclosed.[10,11]

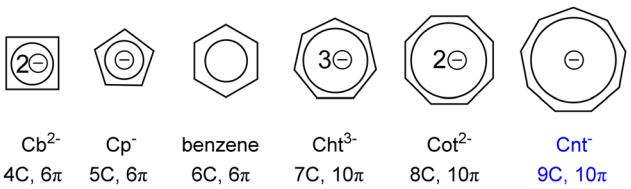


Fig. 1 Aromatic four- to nine-membered carbocycles used as ligands in lanthanide chemistry. For the four-membered ring only a substituted derivate was used as ligand.

It is well-established that the dianionic Cot ligand can serve as a bridging unit to form lanthanide multidecker species.[12–14] In addition, the purely carbon-based seven-membered cycloheptatrienyl trianion has also been employed in organolanthanide chemistry, acting as bridging ligand for inverse sandwich and multidecker compounds.[15–17]

All the carbocycles with ring sizes from four to eight have been utilised in organolanthanide chemistry for over 20 years. The next larger aromatic carbocycle is the nine-membered

[a] *Institute of Inorganic Chemistry (AOC), Karlsruhe Institute of Technology (KIT), Kaiserstr. 12, 76131, Karlsruhe, Germany. E-mail: xiaofei.sun@kit.edu, roesky@kit.edu*
[b] *LCM, CNRS, Ecole Polytechnique, Institut Polytechnique de Paris, 91120 Palaiseau, France*
[c] *Institute of Nanotechnology (INT), Karlsruhe Institute of Technology (KIT), Kaiserstr. 12, 76131, Karlsruhe, Germany*

10π-electron cyclononatetraenyl (Cnt) monoanion, which was only introduced in organolanthanide chemistry in 2017.[18]

The Cnt anion has been known since the 1960s with the corresponding alkali metal salts (Li(Cnt) or K(Cnt)) being synthesized from Cot in a two-step procedure.[19,20] On the basis of their NMR data and the strong UV absorption, their aromatic character has been confirmed. However, synthesising stable complexes with Cnt ligands were found to be extremely challenging due to the large ring size and tendency of skeletal rearrangement.[21,22] Still, Cnt remains attractive as a planar π-ligand in coordination chemistry, especially for generating novel sandwich complexes with ligands beyond the classical smaller ring systems. Early studies on the coordination chemistry of Cnt ligands with transition metal precursors were reported already in the 1970s. The two examples are the synthesis of the heteroleptic compounds, $[(Cp)Ti^{II}(Cnt)]$[23] and $[(Cp)_2Nb^{III}(Cnt)]$,[24] where the spectroscopic observations revealed $\eta^3$- and $\eta^7$-coordination modes for the Ti and Nb compounds, respectively. More recently, in 2009, a tetrapalladium Cnt-based sheet sandwich-type complex was reported and the molecular structure was disclosed.[25]

The Cnt anion can exist as two different isomers, Cnt-*trans* and Cnt-*cis* (Fig. 2). Only recently, the molecular structure of the potassium salt of the Cnt ligand (K(Cnt)) was reported by Nocton[26] and Roesky[27] independently. Depending on the reaction and crystallisation conditions, the outcome of the formation of K(Cnt) slightly differs.[28] Nocton *et al.* reported that recrystallisation of K(Cnt) from diethyl ether, led to single crystals with disorder for the C1 atom (Fig. 3, right), which is linked to the formation of the *cis–cis–cis–cis* isomer (Cnt-*cis*) and the *cis–cis–cis–trans* isomer (Cnt-*trans*) forming a structure resembling a pac-man. Both isomers are present in solution, as evidenced by NMR spectroscopy. For the *cis*-isomer, the monoanionic charge is delocalized over the entire ring, as shown in the fully planar structure and the nearly equivalent C–C bond distances, resulting a $D_{9h}$ symmetry. In contrast, for the *trans* analogue, one of the carbon atoms is inside the ring, and the negative charge is mainly localised over there. Therefore, $C_{2v}$ symmetry is assumed in first approximation. Roesky *et al.* obtained single crystals of K(Cnt) from dimethoxyethane and the structure showed only the Cnt-*cis* form, with the potassium ion exhibiting complete $\eta^9$-coordination towards the ring (Fig. 3, left).

Already in 1973, more than half a century ago, Steitwieser *et al.* attempted to incorporate the Cnt ligand in organolanthanide complexes.[29] They aimed to synthesise the heteroleptic sandwich complex $[(Cnt)Ln^{III}(Cot)]$ (Ln = Ce, Pr, Nd and Sm). However, instead of the expected product, the one-pot reaction between $LnCl_3$, $K_2(Cot)$, and K(Cnt) in THF led to the formation of a new class of mono(cyclooctatetraenediide) compounds, the dimeric chlorides $[Ln^{III}(Cot)(thf)_2Cl]_2$ (**1-Ln**, Ln = Ce, Pr and Sm) (Scheme 1).

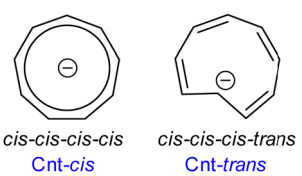


Fig. 2 The two isomers of Cnt.

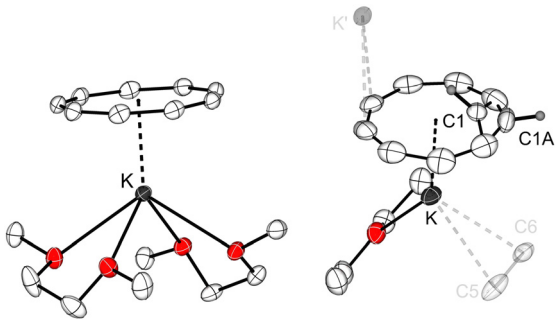


Fig. 3 The molecular structures of $KCnt{\cdot}(dme)_2$ (left) and $KCnt{\cdot}Et_2O$ (right) in the solid state with thermal ellipsoids at 40% probability.†

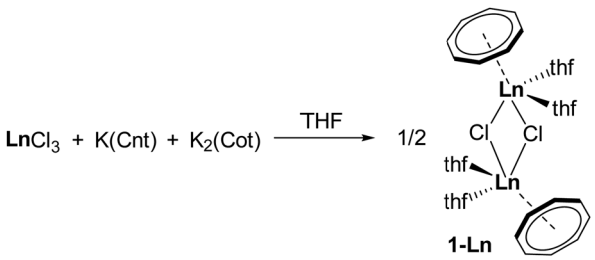


Scheme 1 Reaction of $LnCl_3$, K(Cnt) and $K_2(Cot)$.

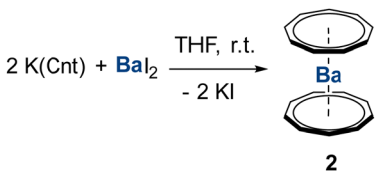


Scheme 2 Synthesis of $[Ba(\eta^9\text{-}Cnt)_2]$ (**2**).

The large diameter (approximately 4.1 Å) of the Cnt ligand appears to be particularly well-suited for metal centres with large ionic radii such as heavy main group metals like Ba, Pb, Bi, and the f-elements. In 2005, Sitzmann *et al.* reported the reaction between K(Cnt) and $BaI_2$ in THF, which resulted in the formation of the homoleptic complex $[Ba(\eta^9\text{-}Cnt)_2]$ (**2**) (Scheme 2).[30] Although no single crystals could be obtained for structure determination, DFT calculations proposed the sandwich-type structure of **2**.

† Reproduced from the CIF file having CCDC numbers of 1861445 ($KCnt{\cdot}Et_2O$), 1894445 ($KCnt{\cdot}(dme)_2$), 1861447 (**3-Sm**), 1544973 (**3-Eu**), 1861450 (**3-Tm**), 1861446 (**3-Tm**), 1894447 (**6-Nd**), 1894448 (**6-Sm**), 2073514, 2073526 (**6-Tb**), 2073516 (**6-Dy**), 2073518 (**6-Ho**), 2073520 (**6-Er**), 2073522 (**6-Tm**), 2073525 (**6-Lu**), 2125024 (**7-La**), 2125026 (**8-Ce**), 2125029 (**9-Er**), 2267628 (**10-La**), 2267629 (**10-Ce**), 2267630 (**11-La**), 2267631 (**11-Ce**), 2267632 (**12-La**), 2113686 (**13-Y**), 2113687 (**13-Gd**), 2113688 (**13-Tb**), 2113689 (**13-Dy**), 2113691 (**13-Er**), 2113690 (**13-Ho**), 2113692 (**13-Tm**), 2370453 (**6-Y-*trans***), 2370455 (**6-La-*trans***), 2370457 (**6-Ce-*trans***), 2370459 (**6-Pr-*trans***), 2370461 (**6-Nd-*trans***), 2370463 (**6-Sm-*trans***), 2370465 (**6-Gd-*trans***), 2370466 (**6-Tb-*trans***), 2370467 (**6-Dy-*trans***), 2370468 (**6-Ho-*trans***).

Further spectroscopic methods (NMR spectroscopy and EI MS) indicated the successful isolation of **2**.

## Lanthanidocenes: divalent bis(cyclononatetraenyl) lanthanide sandwich compounds

In 2017, Nakajima and co-workers made a significant advancement by introducing the Cnt ligand into the coordination sphere of a divalent Ln ion for the first time.[18] They synthesised the homoleptic $Eu^{II}$ sandwich complex $[Eu^{II}(\eta^9\text{-Cnt})]_2$ (**3-Eu**) *via* salt elimination from K(Cnt) and $EuI_2$ in THF (Scheme 3) in extremely low yield (4%). The structure of **3-Eu** was elucidated using single crystal X-ray diffraction (SCXRD) analysis, revealing that the $Eu^{II}$ ion is sandwiched between the two planar Cnt rings (Fig. 4). The 10π-aromatic nature of the Cnt ring is retained as evidenced by the sum of the internal angles (1260°) and the nearly equivalent C–C bond lengths (1.35–1.45 Å, Table 1). The $Eu^{II}$ ion is located at the centre of inversion, which results in a completely linear structure with the Ct–Eu–Ct angle being 180°. The high symmetry was further corroborated by Raman spectroscopy. Complex **3-Eu** shows blue-green emission at 516 nm in toluene at room temperature and at 77 K. This emission is significantly blue-shifted compared to other well-known organoeuropium(II) sandwich complexes since typically, $Eu^{II}$ sandwich complexes with Cp or Cot ligands show red photoluminescence emission at around 600 nm.[31–33] According to DFT calculations, the blue-shift emission of **3-Eu** originates from the energy lowering of the 5d-6s hybridised orbitals and the weak electrostatic potential induced by the Cnt ligands.

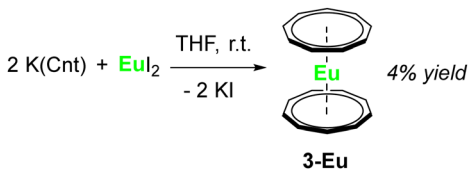


Scheme 3 Synthesis of the homoleptic Eu complex $[Eu^{II}(\eta^9\text{-Cnt})]_2$ (**3-Eu**).

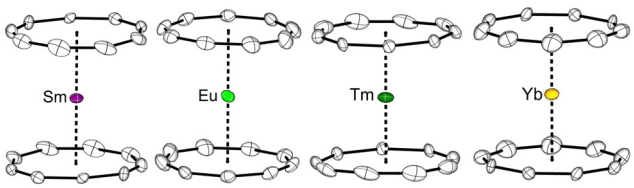


Fig. 4 Molecular structures of $[Ln^{II}(\eta^9\text{-Cnt})_2]$ (**3-Ln**, Ln = Sm, Eu, Tm, Yb) in the solid state with thermal ellipsoids at 40% probability.†

In addition to the experimental findings on **3-Eu**, the electronic structure and photoluminescence properties of **3-Eu** were further analysed *via* quantum computational methods.[34] Ligand-field density functional theory (LFDFT), a DFT-based model incorporating the configuration interaction algorithm through a model Hamiltonian, was employed for the calculations. In the optimized structure of **3-Eu**, both the eclipsed $D_{9h}$ and the staggered $D_{9d}$ conformations, were found to be nearly degenerate, suggesting that the Cnt ligand can freely rotate in the gas phase. The calculated molecular orbital diagram reveals that the Eu 4f orbitals contribute only weakly to the predominantly ionic chemical bonding. Time-dependent DFT (TD-DFT) and LFDFT calculations explained the photoluminescence emission as electric dipole-allowed Eu 4f-5d transitions between the lowest excited $4f^65d^1$ state of the $Eu^{II}$ ion and the $4f^75d^0$ ground state. The low quantum yield in toluene solution at room temperature may be indicative of non-radiative decay caused by strong interactions with solvent molecules.

In 2018, the group of Nocton extended the bis(Cnt) chemistry to other divalent lanthanides, Sm, Tm and Yb.[26] They discovered that both the starting material and the solvent are crucial for the high yield synthesis of $[Ln^{II}(\eta^9\text{-Cnt})_2]$. The *trans*/*cis* isomer mixture of K(Cnt) was necessary for the successful high yield synthesis and when the reactions between K(Cnt) and $LnI_2$ were performed in coordinating solvents (THF, $Et_2O$), the yields remained very low. In contrast, reacting K(Cnt) with $LnI_2$ (Ln = Sm, Eu, Tm, Yb) in toluene with a few drops of THF, crystals of **3-Ln** were obtained in good yields (33–62%) from the toluene filtrate (Scheme 4). $^1H$ NMR spectroscopy of the diamagnetic **3-Yb** and paramagnetic **3-Sm** both indicated the existence of three isomers $[Ln^{II}(Cnt\text{-}cis)_2]$, $[Ln^{II}(Cnt\text{-}trans)_2]$ and $[Ln^{II}(Cnt\text{-}cis)(Cnt\text{-}trans)]$ in solution. Complete isomerisation to the $[Ln^{II}(Cnt\text{-}cis)_2]$ isomers took a few days and the yields were extremely low, which suggested that a better isomerisation solvent is required.

Dissolving the crystals of **3-Yb** in THF led to the formation of the ion pair $[Yb^{II}(Cnt)(thf)_4][Cnt]$ (**4-Yb**) with one coordinated

Table 1 Important metric parameters for **3-Ln**

| | 3-Sm | 3-Eu | 3-Tm | 3-Yb |
|---|---|---|---|---|
| C–C | 1.33(1)–1.47(2) | 1.353(15)–1.448(13) | 1.32(1)–1.47(2) | 1.33(3)–1.43(3) |
| C–C (av.) | 1.39(4) | 1.39(2) | 1.39(4) | 1.39(4) |
| M–C | 2.833(8)–2.958(6) | 2.796(13)–2.957 | 2.736(8)–2.760(8) | 2.74(2)–2.86(2) |
| M–C (av.) | 2.88(3) | 2.87(4) | 2.75(1) | 2.79(3) |
| M–$Cnt_{Ct}$ | 2.061 | 2.065 | 1.91 | 1.932 |
| $Cnt_{Ct}$–$Cnt_{Ct}$ | 4.122 | 4.131 | 3.82 | 3.865 |
| Ring size (max C···C–C) | 4.05 | 4.02 | 4.02 | 4.06 |
| $Cnt_{Ct}$–Ln–$Cnt_{Ct}$ | 180 | 180 | 180 | 180 |

Distances are given in Å and angles are given in deg (°).

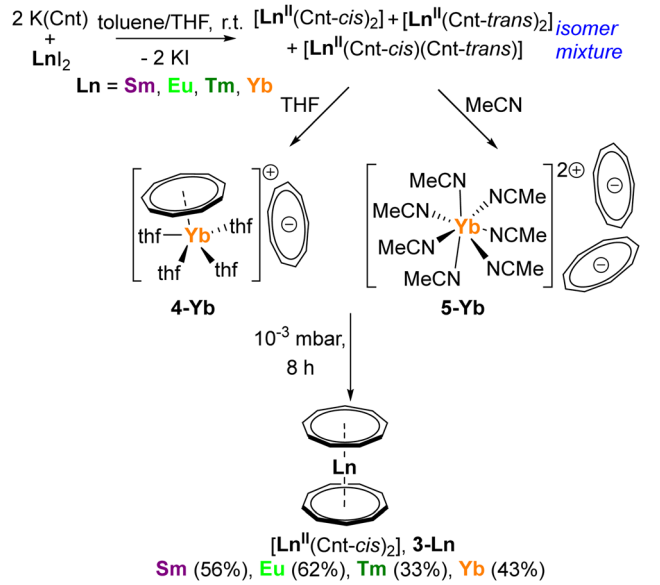


Scheme 4 Synthesis of the homoleptic Ln bis(Cnt) complexes as isomer mixture and the further isomerisation to the $[Ln^{II}(Cnt\text{-}cis)_2]$ complexes **3-Ln**.

and one uncoordinated Cnt ligand (Scheme 4). SCXRD analysis revealed that the coordinated one exhibits a 1 : 1 ratio disorder between the *trans* and *cis* forms, while the uncoordinated one consists entirely of the *cis* isomer. Treating the crystals of **3-Yb** with acetonitrile resulted in the full decoordination of the two Cnt ligands from the $Yb^{II}$ centre and the formation of the ion pair $[Yb^{II}(CH_3CN)_7][Cnt]_2$ (**5-Yb**). The $Yb^{II}$ ion exhibits a distorted pentagonal bipyramidal geometry and the two Cnt anions are in *cis* configuration. A pivotal step to get access to pure $[Yb^{II}(Cnt\text{-}cis)_2]$ is to dry the crystals of **5-Yb** under $10^{-3}$ mbar vacuum for 8 h (Scheme 4). Applying similar procedures for the other divalent Ln complexes also led to the clean formation of $[Ln^{II}(Cnt\text{-}cis)_2]$ (**3-Ln**, Ln = Sm, Eu and Tm).

**3-Sm**, **3-Tm** and **3-Yb** are isomorphous to the previously reported **3-Eu**. The high symmetry of the sandwich structures can be reflected from their crystallographic features as the $Ln^{II}$ atoms are positioned at the centre of inversion, leading to rigorously linear sandwich motifs. Additionally, the Cnt rings exhibit disorder with altering stacked $D_{9h}$ and eclipsed $D_{9d}$ symmetry, which could potentially result in interesting spectroscopic properties. For example, very recently, Vitova *et al.* investigated the electronic structure of $[Sm^{II}(\eta^9\text{-Cnt})_2]$ (**3-Sm**) by valence band high-energy resolution resonant inelastic X-ray scattering (VB-RIXS), high-resolution X-ray absorption near-edge structure (HR-XANES) and quantum chemical computations. The results demonstrated that the ionic bond of **3-Sm** can be photo-modulated and the Sm–C bond covalency increases by transfer of the $Sm^{II}$ 4f electrons to the 5d orbitals.[35] This change leads to a reconfiguration of **3-Sm** with a detectable contraction in Sm–C bond lengths and increased disorder in the local $Sm^{II}$ coordination environment.

## Super sandwich complexes: heteroleptic trivalent lanthanide complexes

Soon after the report on the homoleptic bis(Cnt) lanthanidocenes by Nocton,[26] Roesky *et al.* introduced a new class of super sandwich complexes, which are heteroleptic sandwich compounds comprising both the Cot and Cnt ligands, $[(Cnt)Ln^{III}(\eta^8\text{-Cot})]$.[27] While the majority of the previously reported classical sandwich compounds consists the small five-membered Cp ring, the term super sandwich compounds is introduced to define sandwich complexes in which the central metal atom is coordinated by ligands with more than 16 carbon atoms in total. As already mentioned, the synthesis of $[(Cnt)Ln^{III}(\eta^8\text{-Cot})]$ was initially attempted by Streitwieser *et al.* in 1973 using a one-pot procedure from the chloride precursors (Scheme 1),[36] but only the Cot-functionalised lanthanide chlorides were isolated at that time. In 2019, Roesky *et al.* reported the successful synthesis of these heteroleptic sandwich complexes using iodide-based Ln compounds as starting materials.

The synthesis began with the preparation of the half-sandwich compounds $[(\eta^8\text{-Cot})Ln^{III}I(thf)_n]$ (Ln = Nd, Sm, Dy and Er; $n$ = 2 for Sm, Dy, Er, $n$ = 3 for Nd) from cyclooctatetraene, Ln metal and iodine, following a slightly modified procedure by Mashima *et al.*[37] Refluxing K(Cnt) with $[(\eta^8\text{-Cot})Ln^{III}I(thf)_n]$ in toluene yielded the super sandwich complexes **6-Ln** (Ln = Nd, Sm, Dy and Er) in moderate yields of 31–36% after crystallisation from toluene (Scheme 5). Despite some disorder in the crystal structures, the **6-Nd** and **6-Sm** complexes exhibit perfect sandwich-type structure motifs with $\eta^8$-coordinated Cot and $\eta^9$-coordinated Cnt rings in nearly ideal coplanar arrangement (Fig. 5). Notably, the smaller Cot ligand is much closer to the $Ln^{III}$ centre compared to the larger Cnt ligand, which is mostly attributed to the dianionic charge of Cot which results in a stronger electrostatic attraction. Greater disorder was found in the crystal structures of the smaller lanthanides, **6-Dy** and **6-Er**, and detailed investigation of the structures were published later.[38]

It is known that equatorial ligands are beneficial for enhancing the magnetic anisotropy of $Er^{III}$ due to the prolate nature of its highest $m_J$ state. **6-Er** exhibited single molecule magnet (SMM) behaviour, characterised by an open butterfly-like

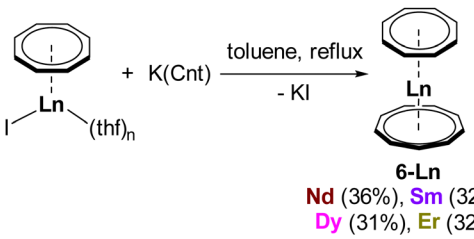


Scheme 5 Synthesis of the heteroleptic sandwich complexes $[(Cnt)Ln^{III}(\eta^8\text{-Cot})]$ (**6-Ln**, Ln = Nd, Sm, Dy and Er) from $[(\eta^8\text{-Cot})Ln^{III}I(thf)_n]$ and K(Cnt).

 

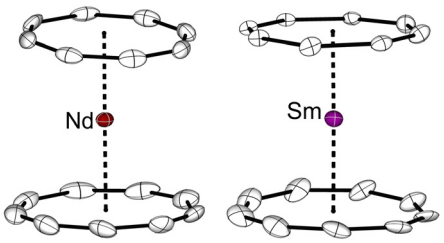


Fig. 5 Molecular structures of **6-Nd** (left) and **6-Sm** in the solid state with thermal ellipsoids at 40% probability.†

magnetic hysteresis loop up to 10 K, which was well-reproduced by CASSCF calculations. The magnetic properties of **6-Er** indicate that the combination of the Cot/Cnt ligands induces a strong equatorial ligand field. Conversely, **6-Dy** showed less promising magnetic properties since the highest $m_J$ state with oblate shape is best to be stabilised by axial ligands, instead of the equatorial Cot/Cnt ligands.

Roesky and Nocton further expanded the chemistry of the super sandwich complexes to additional late lanthanides, Tb, Ho, Tm and Lu.[38] In an alternative synthesis to the one described earlier (Scheme 5), the reactions between the half-sandwich starting material [($\eta^8$-Cot)Ln$^{III}$I(thf)$_n$)] and K(Cnt) were performed in acetonitrile/toluene mixture at room temperature (Scheme 6). For the smallest element Lu, the synthesis was optimised by refluxing the borohydride precursor [($\eta^8$-Cot)Lu$^{III}$(BH$_4$)(thf)$_2$)] and K(Cnt) in toluene (Scheme 6). The analogues Yb$^{III}$ sandwich complex was not formed due to reduction by the Cot ligand. Sufficient drying before recrystallisation from toluene is crucial in order to remove the coordinating solvent molecules (THF or acetonitrile), as incomplete removal results in crystal structures with partially coordinated solvent molecules and lower hapticities than $\eta^9$ for the Cnt ligands.

The properties of **6-Ln** were analysed in toluene-d$_8$ solution using $^1$H NMR spectroscopy. Depending on the nature of the Ln$^{III}$, the spectra showed either two broad or well-defined sharp singlet signals for the Cnt and Cot protons at room temperature. Complex **6-Lu** exhibited no fluxional behaviour from

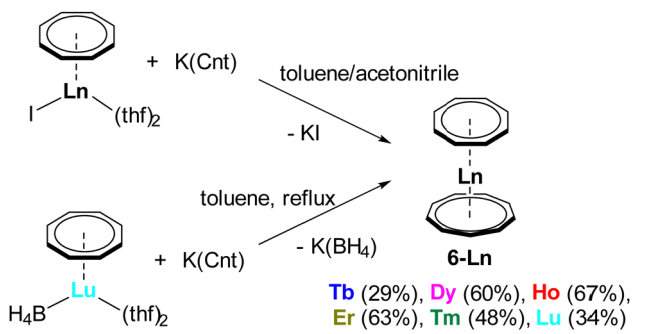


Scheme 6 Synthesis of the heteroleptic sandwich complexes [(Cnt)Ln$^{III}$($\eta^8$-Cot)] (**6-Ln**, Ln = Tb, Dy, Ho, Er, Tm and Lu) from [($\eta^8$-Cot)Ln$^{III}$I(thf)$_n$)] (Tb, Dy, Ho, Er, and Tm) and K(Cnt) in toluene/acetonitrile mixture or from [($\eta^8$-Cot)Lu$^{III}$(BH$_4$)(thf)$_2$)] and K(Cnt) in toluene under reflux.

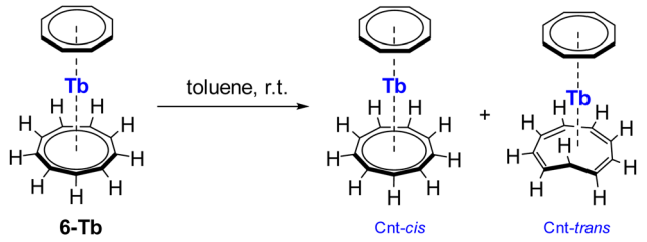


Scheme 7 Isomerisation of **6-Tb** in toluene at room temperature.

−80 °C to 80 °C. Interestingly, for the **6-Tb** complex, the Cnt ligand consisted initially of purely *cis*-configuration, but it partially isomerised to **6-Tb**′ over the course of several days (Scheme 7). This isomerisation process was followed by NMR spectroscopy and the amount of **6-Tb**′ increased over the time. **6-Tb**′ consists of an $\eta^8$-coordinating Cot ring and the Cnt-*trans* ligand, in which one of the carbon atoms is inside of the ring. This configuration has been known since the 1960s and was recently discussed for the divalent lanthanidocene complexes **3-Ln**.[26,28,39,40] Complex **6-Tb**′ with Cnt-*trans* was also observed in the solid-state structure. Depending on the reaction temperature and crystallisation method, single crystals of the Tb$^{III}$ sandwich complex were found to contain either only the Cnt-*cis* isomer or a disorder of Cnt-*cis*/Cnt-*trans* isomers (Fig. 6). When the reaction was performed in toluene/acetonitrile mixture at room temperature, the isolated crystals from toluene consist of solely the Cnt-*cis* isomer.

Synthesising the Tb$^{III}$ species in hot toluene resulted in a mixture of sandwich compounds with Cnt-*cis* and Cnt-*trans* isomers. Among all **6-Ln** complexes, this isomerisation has only been detected for the Tb$^{III}$ species.

Molecular structures of all **6-Ln** complexes were studied by SCXRD analyses. Among the late lanthanides (Ln = Tb, Dy, Ho, Er, Tm and Lu) (Fig. 6), only the Tb$^{III}$ complex **6-Tb** displayed two almost coplanar rings with the Cnt ligand in the $\eta^9$-coordination mode (Fig. 6 left). As for the smaller lanthanides, Dy$^{III}$ to Lu$^{III}$, the solid-state structures exhibit significant disorder, with the structure of **6-Lu** being the most disordered one (Fig. 7). The disorder in the structures posed challenges in the refinement. The Ln is positioned close to the centre of inversion with 0.5 occupancy, and a 0.5/0.5 disorder of both the Cot/Cnt rings were found. The optimal approach to model this disorder problem is to maintain the Cot ring relatively planar,

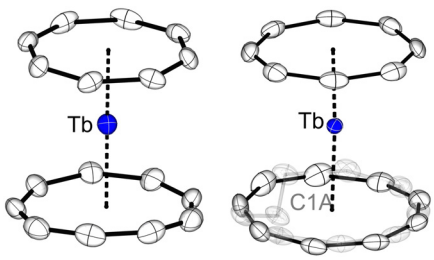


Fig. 6 Molecular structures of [(Cnt)Tb$^{III}$($\eta^8$-Cot)] with purely Cnt-*cis* (left) and Cnt-*cis*/Cnt-*trans* disorder (right) in the solid state with thermal ellipsoids at 40% probability.†

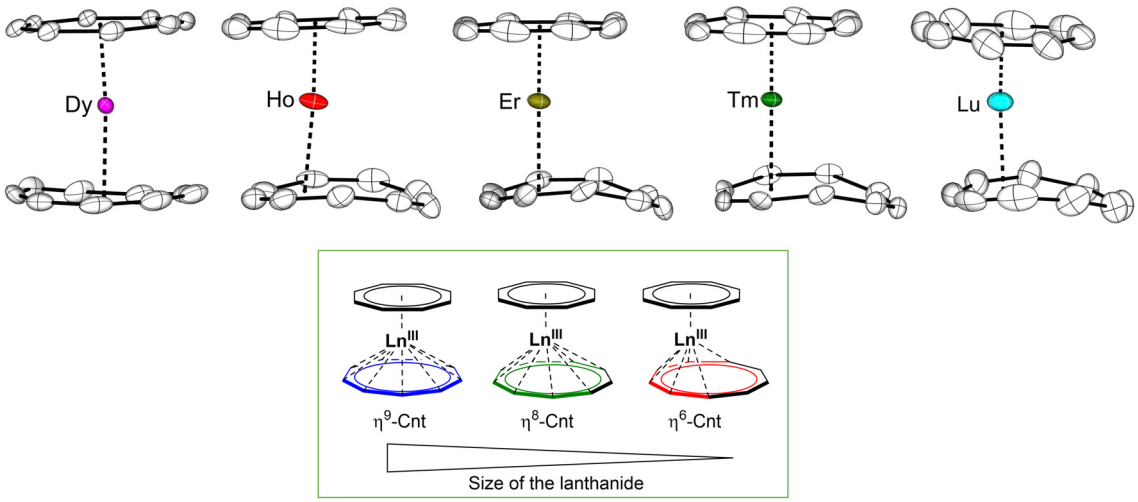


Fig. 7 Top: Molecular structures of [(Cnt)$Ln^{III}$($\eta^8$-Cot)] (**6-Ln**, Ln = Dy, Ho, Er, Tm and Lu) in the solid state with thermal ellipsoids at 40% probability.† Bottom: Representation of size-dependent coordination modes of the Cnt ligand in the [(Cnt)$Ln^{III}$($\eta^8$-Cot)] (**6-Ln**) sandwich complexes.

which is consistent with its typical planarity reported in the literature. The $Ct_{Cot}$–$Ln^{III}$ distances nicely correlate to the lanthanide contraction, gradually decreasing from $Ct_{Cot}$–$Tb^{III}$ (1.804 Å) to $Ct_{Cot}$–$Lu^{III}$ (1.653 Å). In contrast, the Cnt exhibited some degree of deformation from planarity, which is indicative for a lower hapticity. A careful evaluation of the structural metrics revealed that from $Tb^{III}$ to $Lu^{III}$, the lanthanide contraction results in a transition of the hapticity of the Cnt ligand from $\eta^9$ (Tb) to $\eta^6$ (Lu) and meanwhile the Cnt ring shows greater deviation of planarity for the smaller $Ln^{III}$ ions (Fig. 6 and 7). Furthermore, different measurement temperatures also have slight effect on the coordination mode.

Magnetic measurements of **6-Tb**, **6-Dy**, **6-Ho** and **6-Tm** showed that the large aromatic Cnt ligand is well suited for the prolate $Er^{III}$ and $Tm^{III}$ ions. However, none of the four compounds behave as SMMs, which is different compared to the erbium congener **6-Er**. *Ab initio* computational studies indicated that the deviation from planarity and the reduced hapticity of the Cnt do not significantly impact the overall anisotropy in the case for the prolate ions but influence the composition and ratio of mixed $m_J$ states in non-adapted oblate ions.

## Molecular lanthanide switches based on the lability of the cyclononatetraenyl ligand

Based on the lability of Cnt ligands in the presence of coordinating solvents, Roesky *et al.* reported that the heteroleptic sandwich complexes [(Cnt)$Ln^{III}$($\eta^8$-Cot)] (**6-Ln**) can be used as tools for reversible manipulation of magnetic and photoluminescent properties.[41] Upon addition of THF to the solid samples of [(Cnt)$Ln^{III}$($\eta^8$-Cot)] (**6-Ln**, Ln = La, Ce, Nd, Tb and Er), a colour change occurred immediately, indicating changes in chemical environments of the $Ln^{III}$ metals (Scheme 8). Crystallisation from hot THF solution yielded single crystals for all the five complexes. Depending on the size of the $Ln^{III}$ metal, the obtained products could be classified into three different categories. For the larger $La^{III}$ and $Ce^{III}$ metals, coordination of THF led to the formation of the neutral complexes [($\eta^4$-Cnt)$Ln^{III}$(thf)$_2$($\eta^8$-Cot)] (**7-Ln**, Ln = La and Ce, category I). These neutral species feature a planar $\eta^8$-Cot ligand and an $\eta^4$-coordinated, heavily bent Cnt ligand. In addition, two THF molecules are coordinated to the central metal ions. For the large and medium-sized $Ln^{III}$ ions, Ce, Nd and Tb, the ionic products [$Ln^{III}$(thf)$_n$($\eta^8$-Cot)][Cnt] (**8-Ln**, Ln = Ce, Nd and Tb, category II) were obtained. The Cnt ligand is completely replaced by four THF molecules and act as non-coordinating anion. Interestingly, for cerium, THF coordination can lead to formation of both the neutral species **7-Ce** (category I) and the ionic species **8-Ce** (category II), depending on the crystallisation temperature. For the smallest $Er^{III}$ ion, the ionic complex [$Er^{III}$(thf)$_3$($\eta^8$-Cot)][Cnt] (**9-Er**, category III) with three coordinated THF molecules was formed. The lower coordination number is likely due to the smaller ionic radius of $Er^{III}$ in comparison to the other lanthanides ($Ce^{III}$, $Nd^{III}$ and $Tb^{III}$). This solvation process was entirely reversible, drying the products **7-Ln**–**9-Ln** under dynamic vacuum gave the corresponding starting materials [(Cnt)$Ln^{III}$($\eta^8$-Cot)] (**6-Ln**, Scheme 8). This reversible process was repeatable and can be controlled by external stimuli such as pressure or temperature, enabling selective modification of the ligand sphere through solid-to-solid transformation. This solvation/desolvation process was nicely demonstrated by Raman spectroscopy in an inert vessel using the $Ce^{III}$ complex [(Cnt)$Ce^{III}$($\eta^8$-Cot)] (**6-Ce**) as a model system. A Nd:YAG laser was used as an external heating source. The laser beam was capable of removing THF from the sample in a spatially resolved manner and upon cooling the process was reverted.

Utilising these reversible properties, the $Ce^{III}$ and $Tb^{III}$ complexes **6-Ln** can act as switchable luminophores. Significant differences were observed in the photoluminescence

 

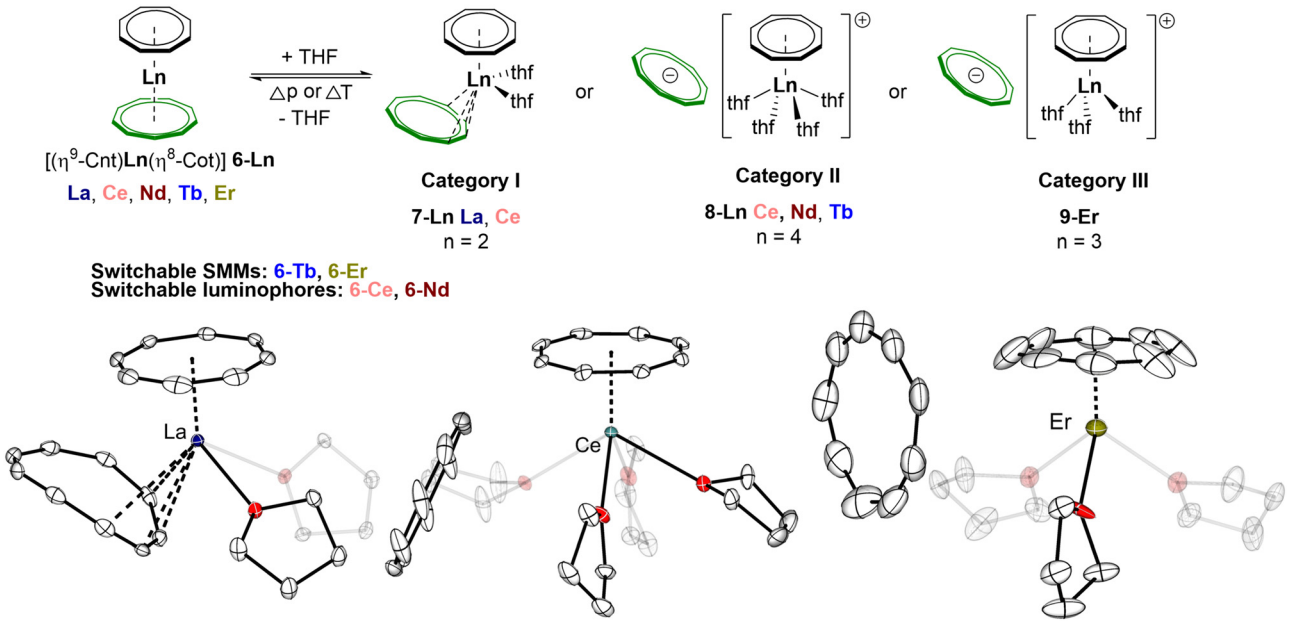


Scheme 8 Top: Schematic representation of the reversible solvation process in the $[(\eta^9\text{-Cnt})Ln^{III}(\eta^8\text{-Cot})]/[Ln^{III}(thf)_n(\eta^8\text{-Cot})][Cnt]$ (Cat I, $n$ = 2, Cat II, $n$ = 4, Cat III, $n$ = 3) systems. Bottom: Molecular structures of **7-La**, **8-Ce** and **9-Er** in the solid state with thermal ellipsoids at 40% probability.

properties of the solvent-free neutral sandwich compounds $[(Cnt)Ln^{III}(\eta^8\text{-Cot})]$ (**6-Ln**) compared to the solvated ionic analogues $[Ln^{III}(thf)_4(\eta^8\text{-Cot})][Cnt]$ (**8-Ln**). While **6-Ln** did not show significant light emission, the ionic versions **8-Ln** exhibited intense photoluminescence upon UV-light irradiation. The two forms were easily switched by adding THF to **6-Ln** and applying vacuum to **8-Ln**. While the emission properties changed, the colours of the respective crystalline materials also changed, which clearly indicated the successful solvation and desolvation.

Besides acting as switchable luminophores, the magnetic properties of the $Er^{III}$ and $Nd^{III}$ complexes **6-Er** and **6-Nd** showed significant different SMM behaviours after THF addition. For instance, the neutral Er complex $[(Cnt)Er^{III}(\eta^8\text{-Cot})]$ (**6-Er**) exhibits good SMM behaviour with high energy barriers, whereas the THF-solvated analogue **9-Er** showed faster relaxation and lower barriers. In contrast to **6-Er** and **9-Er**, the Nd system showed more distinct behaviour. While $[(Cnt)Nd^{III}(\eta^8\text{-Cot})]$ (**6-Nd**) behaved as an SMM, the SMM character was entirely shut off upon solvation and formation of **8-Nd**. Theoretical calculations further provided explanation of the different magnetic behaviour of these compounds. The almost pure character $m_J$ ground states of **6-Nd** accounted for its SMM character. Computational analysis also explained the lack of SMM character of **8-Nd**, which is attributed to the pseudo-planar anisotropy of its ground doublet state with highly mixed $m_J$ values.

## Photo-isomerisation of the cyclononatetraenyl ligand and its rare-earth complexes

The Cnt ligand can exist in two isomeric forms (Fig. 2), Cnt-*cis* and Cnt-*trans*. Both isomers are known to exist as free ligands and in some lanthanide complexes. According to the original ligand synthesis reported by Katz *et al.* in 1963, the *cis*-isomer is formed when treating the dipotassium cyclooctatetraenediide with either dichloromethane or dichloromethylmethylether.[19] In an alternative synthetic pathway reported by Lalancette *et al.* in the same year, the *trans*-isomer is favoured.[20] Boche's studies in 1978 detailed this isomerisation,[28] highlighting the *trans*-to-*cis* isomerisation and indicating that the *cis*-form is the thermodynamically more stable isomer. Besides the early reports on the Cnt ligand, the different isomers of the Cnt ligand have also been observed during the synthesis of some divalent and trivalent rare-earth compounds (*vide supra*).[26,38] The serendipitous observation of slow *cis*-to-*trans* isomerisation of Cnt ligand in $[(Cnt)Tb^{III}(\eta^8\text{-Cot})]$ (**6-Tb**) reported by Nocton and Roesky,[38] contradicts the classical thermodynamics for the pure ligand isomerisation reported by Boche. Boche's pioneering work also briefly suggested that light might induce the isomerisation of the Cnt ligand.[28] This led to an in-depth study of this phenomenon for the Cnt ligand and in related rare-earth complexes, which was very recently reported by Nocton.[42]

Spontaneous isomerisation of Cnt-*trans* to Cnt-*cis* occurs at room temperature, but by maintaining the temperature at 233 K, a *trans*:*cis* ratio of 80 : 20 can be achieved. By performing the synthesis under light exclusion, this ratio can be increased to 95 : 5. Instead of the mixture of different isomers (Scheme 4), by having the Cnt-*trans* ligand (K(Cnt-*trans*)) in high purity in hand, the reaction between $SmI_2$ and K(Cnt-*trans*) was performed under light protection in toluene, resulting in the formation of pure $[Sm(Cnt\text{-}trans)_2]$ (**3-Sm-*trans***, Scheme 9). Although pure **3-Sm-*trans*** was obtained according to NMR spectroscopy, crystallisation always led to a mixture of different isomers, likely due to the unavoidable slow isomerisation during the crystallisation process and the solubility differences between the *trans* and *cis* isomers.

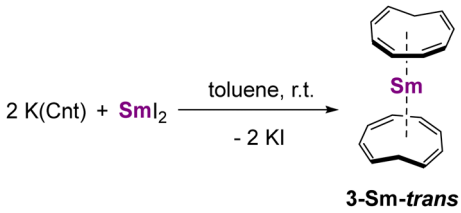


Scheme 9 Synthesis of [Sm(Cnt-*trans*)$_2$] (**3-Sm-*trans***).

Furthermore, to deepen the understanding of how light and solvent affect the outcome of the synthesis of [(Cnt)Ln$^{III}$($\eta^8$-Cot)] (**6-Ln**) and to obtain a series of heteroleptic sandwich complexes analogues to **6-Ln** with the Cnt either in purely *cis* or *trans* form, the synthesis was carefully performed under different conditions. Analogous to the synthesis described earlier (Scheme 6), when reacting K(Cnt) and [($\eta^8$-Cot)Ln$^{III}$I(thf)$_n$)] (Ln = Y, La, Ce, Pr, Nd, Sm, Gd, Tb, Dy, Ho; $n$ = 2, 3) in a toluene/acetonitrile mixture under ambient light, **6-Ln** complexes with pure Cnt-*cis* were obtained. Alternatively, performing the reaction in non-coordinating solvent (toluene) under light protection using K(Cnt-*trans*) and [($\eta^8$-Cot)Ln$^{III}$I(thf)$_n$)] (Ln = Y, La, Ce, Pr, Nd, Sm, Gd, Tb, Dy, Ho; $n$ = 2, 3), crystalline products with a high ratio of [(Cnt-*trans*)Ln$^{III}$($^8$-Cot)] (**6-Ln-*trans***) were obtained from concentrated toluene solutions in all cases (Fig. 8). The *trans*:*cis* ratios were analysed using $^1$H NMR spectroscopy and SCXRD analysis. For the obtained crystals of **6-Ln-*trans***, the *trans*:*cis* ratio varied depending on the rare-earth metal ion. Crystals of the Tb, Dy and Ho complexes consisted of 100% of the *trans* isomer, while the ratios for the other rare-earth metals were 71% (Gd), 69% (Sm), 58% (Nd), 55% (Pr), 50% (Ce), 25% (La) and 73% (Y), respectively. The Ln–C distances for both the Cot and Cnt rings, as well as the Ln–C1 distance decrease along the lanthanide series, with a notable exception in **6-Ho**, due to changes in the coordination mode (Table 2).[38] Solid structures only represent the portion of the product mixture that crystallised. Since Cnt-*trans* is more soluble than Cnt-*cis*, the observed ratios according to XRD analyses are not accurate. Therefore, further solution analysis was performed. Complex **3-Sm-*trans*** showed five signals in 2:2:2:2:1 molar ratio in the $^1$H NMR spectrum, consistent with the Cnt-*trans* having $C_{2v}$ symmetry in solution. For the series of **6-Ln-*trans*** complexes, both isomers were identified according to the $^1$H NMR spectra. Using that method allowed the correct identification of both isomers in solution.

The photo-isomerisation of the Cnt ligand, as well as complex **3-Sm** and **6-Ln**, were studied in detail. The solutions were directly irradiated in NMR tubes at different wavelengths, and the resulting isomer ratios were quantified using $^1$H NMR spectroscopy. The isomerisation of the Cnt ligand from Cnt-*trans* to Cnt-*cis* was monitored using 427 nm irradiation, showing a pseudo-first-order reaction rate, with complete conversion achieved after

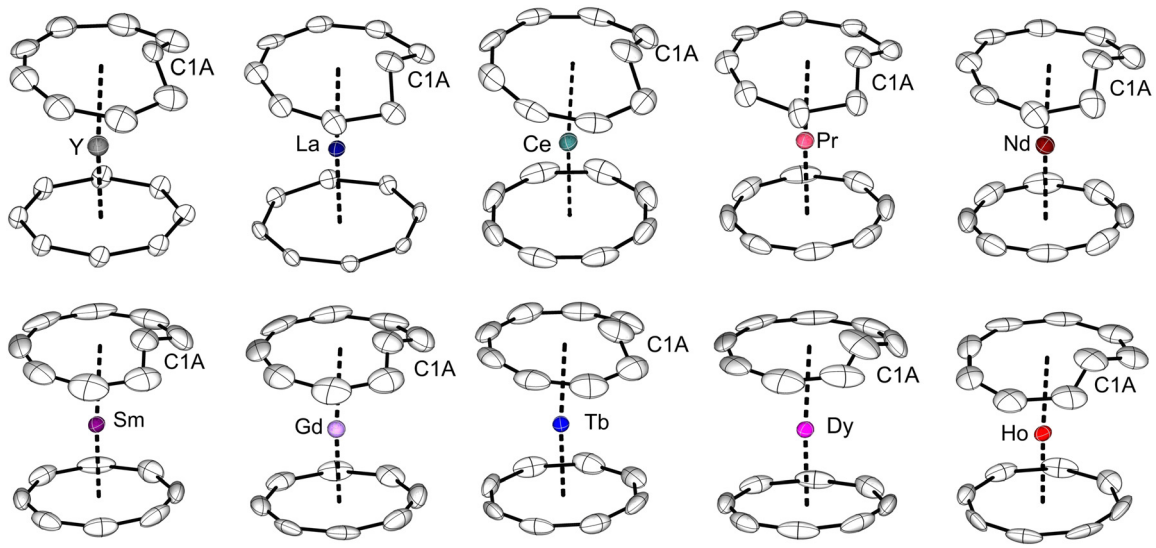


Fig. 8 Molecular structures of [(Cnt-*trans*)Ln$^{III}$($\eta^8$-Cot)] (**6-Ln-*trans***, Ln = Y, La, Ce, Pr, Nd, Sm, Gd, Tb, Dy, Ho) in the solid state with thermal ellipsoids at 40% probability.†

Table 2 Important metric parameters for **6-Ln-*trans***

| | 6-Y-trans | 6-La-*trans* | 6-Ce-*trans* | 6-Pr-*trans* | 6-Nd-*trans* | 6-Sm-*trans* | 6-Gd-*trans* | 6-Tb-*trans* | 6-Dy-*trans* | 6-Ho-*trans* |
|---|---|---|---|---|---|---|---|---|---|---|
| Ln–$C_{Cot}$ (av.) | 2.542(8) | 2.694(4) | 2.54(4) | 2.636(6) | 2.625(9) | 2.595(6) | 2.570(7) | 2.552(10) | 2.541(5) | 2.478(7) |
| Ln–$C_{Cnt}$-C8 (av.) | 2.806(9) | 2.905(8) | 2.881(15) | 2.86(2) | 2.87(2) | 2.833(8) | 2.826(9) | 2.818(11) | 2.802(8) | 2.792(9) |
| Ln–C1A | 2.657(10) | 2.851(16) | 2.750(12) | 2.749(15) | 2.79(2) | 2.687(13) | 2.703(17) | 2.664(16) | 2.660(9) | 2.673(11) |
| Ln–$C_{Cnt}$ (av.) | 2.776(9) | 2.894(10) | 2.85(1) | 2.84(2) | 2.85(2) | 2.804(9) | 2.801(11) | 2.787(13) | 2.774(8) | 2.768(9) |

Distances are given in Å.

 

Table 3 Summary of the *trans* ratios obtained from **6-Y-*trans*** to **6-Lu-*trans*** during the synthesis by $^1$H NMR, XRD analysis and the ratio at PSS

| | **6-Y-*trans*** (%) | **6-La-*trans*** (%) | **6-Ce-*trans*** (%) | **6-Sm-*trans*** (%) | **6-Tb-*trans*** (%) | **6-Dy-*trans*** (%) | **6-Lu-*trans*** (%) |
|---|---|---|---|---|---|---|---|
| NMR | 61 | 55 | 79 | 89 | 87 | 75 | 0 |
| XRD | 73 | 25 | 50 | 69 | 100 | 100 | 0 |
| PSS 370 nm | 96 | 93 | 97 | 64 | 78 | 76 | 69 |
| PSS 370 nm | 99 | 98 | 100 | 52 | 79 | 75 | 71 |
| PSS 427 nm | 97 | 99 | 94 | 28 | 50 | 48 | 29 |
| PSS 440 nm | 95 | 99 | 86 | 23 | 39 | — | 20 |
| PSS 450 nm | — | — | — | — | — | 33 | — |
| PSS 467 nm | 92 | 99 | 64 | 13 | 28 | — | 11 |
| PSS 525 nm | 90 | 98 | 88 | 12 | 1 | 6 | 9 |

5 min. Under 427 nm irradiation, complex **3-Sm-*trans*** isomerised *via* the intermediate **3-Sm-*trans*–*cis*** to **3-Sm** within 30 min, with both steps showing pseudo-first-order reaction rates. However, complete photochemical analysis was not conducted for the isomerisation of the Cnt ligand and the **3-Sm** complex.

The photo-isomerisation of the heteroleptic complexes **6-Ln** and further analysis are more challenging due to strong paramagnetic nature of some lanthanides and overlapping signals of the isomers in the $^1$H NMR spectra. For the compounds where integration was possible, irradiation at different wavelengths produced different *trans*:*cis* ratios (Table 3). Kinetic studies on complex **6-Sm** showed that the photo-stationary state (PSS) was reached after 30 min of irradiation, meaning the *trans*:*cis* ratio no longer changed. This behaviour was studied for all the **6-Ln** (Ln = Y, La, Ce, Sm, Tb, Dy and Lu) complexes, and it varied depending on the irradiation wavelengths and metal ion. For the early lanthanides La and Ce, as well as Y, different wavelengths showed minor changes in the PSS ratios, consistently favouring the *trans* isomers (Table 3). In contrast, for the later lanthanides, Sm, Tb, Dy and Lu, the *trans* ratios showed significant differences depending on the irradiation wavelengths. Under high-energy irradiation, the *trans* isomers were favoured while under low energy irradiation, the *cis* isomers were preferentially formed. These variations might be explained by differences in the energy barriers and absorption cross-sections of the isomers. The photo-isomerisation process of these systems is complex, DFT and TD-DFT were performed to offer a preliminary orbital explanation.

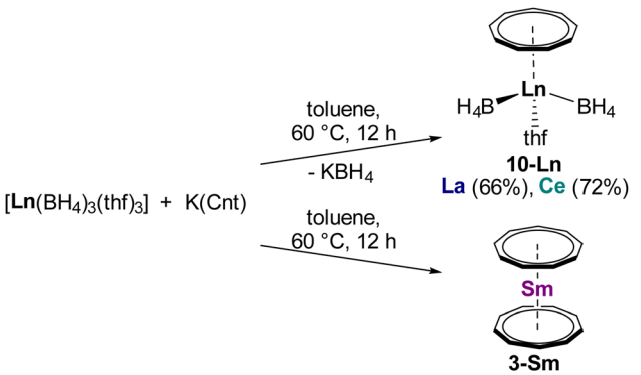


Scheme 10 Synthesis of the half sandwich complexes **10-Ln** and reaction between $[Sm^{III}(BH_4)_3(thf)_3]$ and K(Cnt).

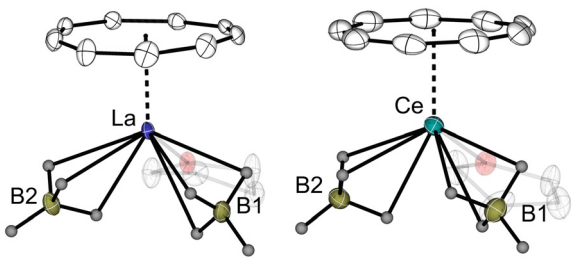


Fig. 9 Molecular structures of $[(\eta^9\text{-Cnt})Ln^{III}(BH_4)_3(thf)]$ (**10-Ln**, Ln = La, Ce) in the solid state with thermal ellipsoids at 40% probability.†

## Mono(cyclononatetraenyl) half-sandwich complexes

Very recently, Roesky *et al.* reported the first examples of trivalent lanthanide half-sandwich complexes comprising the planar Cnt ligand.[43] Reaction of the well-soluble tris(borohydride) precursors $[Ln^{III}(BH_4)_3(thf)_3]$ (Ln = La, Ce) and K(Cnt) in equimolar ratio at 60 °C in toluene led to the formation of the half-sandwich compounds **10-Ln** (Ln = La, Ce; Scheme 10). This procedure only succeeded in the isolation of the respective compounds with the early and large lanthanides, $La^{III}$ and $Ce^{III}$. Attempts to synthesise the corresponding $Sm^{III}$ complex using $[Sm^{III}(BH_4)_3(thf)_3]$ and K(Cnt) yielded the divalent complex $[Sm^{II}(\eta^9\text{-Cnt})_2]$ (**3-Sm**) along with unidentifiable side products. Further attempts to achieve the mono(Cnt) compounds with the even smaller lanthanides $Dy^{III}$ and $Er^{III}$ were also unsuccessful. Such different outcomes may be explained by the different ionic radii of the respective lanthanides.

Single crystals of **10-Ln** were obtained from the concentrated toluene solutions at −10 °C in 66% and 72% yields for **10-La** and **10-Ce.** The two isostructural complexes with the general formula of $[(\eta^9\text{-Cnt})Ln^{III}(BH_4)_3(thf)]$ exhibit three-legged piano-stool-type structure motifs (Fig. 9). In these structures, the $Ln^{III}$-ions are being $\eta^9$-coordinated by the planar Cnt ring, two terminal $BH_4$ ligands and one THF molecule. The molecular structures resemble similarities to that of the $Ln^{III}$ half sandwich borohydride compounds with the sterically-demanding silyl-functionalized Cot ligand.[44] The binding mode of the Cnt ring was further confirmed by Raman spectroscopy, which show clearly

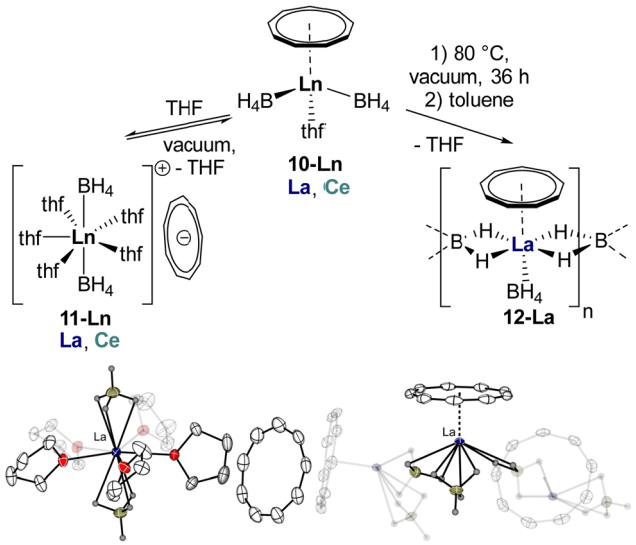


Scheme 11 Top left: Equilibrium between complexes **10-Ln** and **11-Ln** upon reaction with THF or drying under vacuum. Right: Polymeric complex **12-La** formed after drying **10-La** at 60 °C under vacuum and crystallisation from toluene. Bottom: Molecular structures of **11-La** and **12-La** in the solid state with thermal ellipsoids at 40% probability.†

assignable characteristic ring vibrations ($\nu_{asym}(\eta^9\text{-Cnt})$ = 1520 $cm^{-1}$ (**10-La**), 1522 $cm^{-1}$ (**10-Ce**); $\nu_{sym}(\eta^9\text{-Cnt})$ = 678 $cm^{-1}$ (**10-La**), 679 $cm^{-1}$ (**10-Ce**)) and ($\nu$(Ln-Cnt) = 145 $cm^{-1}$ (**10-La**), 140 $cm^{-1}$ (**10-Ce**)). In the $^1$H NMR spectra, a singlet signal was detected for the Cnt protons at 7.01 ppm for the diamagnetic **10-La** and at 5.41 ppm for the paramagnetic **10-Ce.** The $BH_4$ proton signals were found at 1.26–0.61 ppm for **10-La** and at 35.2 ppm for **10-Ce.**

Solvation experiments revealed that dissolving **10-La** and **10-Ce** in warm THF led to the formation of the ionic species $[Ln^{III}(BH_4)_2(thf)_5][Cnt]$ (**11-Ln**) (Ln = La, Ce, Scheme 11), in which the Cnt ligands decoordinate from the $Ln^{III}$ ions. Instead, five THF molecules are coordinated to the metal centres in their equatorial positions. The two terminal $BH_4$ anions coordinate to the $Ln^{III}$ centres in their axial positions, resulting in cationic parts that exhibit pentagonal bipyramidal geometries. A similar displacement of the Cnt ligand by THF was also found for the super sandwich complexes $[(Cnt)Ln^{III}(\eta^8\text{-Cot})]$ (**6-Ln**).[41] These results clearly demonstrate the labile coordination between the $Ln^{III}$ ions and the Cnt ligand, in comparison to the strong coordination with the hard THF donor. Additionally, the Cnt is also weaker bound to the $Ln^{III}$ ions compared to the smaller Cp ligand, as these compounds do not dissociate in THF. Interestingly, the displacement of Cnt by THF from **10-Ln** to **11-Ln** is fully reversible as the half-sandwich compounds **10-Ln** were formed again after drying the crystals of **11-Ln** under vacuum. This was proven by Raman spectroscopy of the dried crystals, indicating their potential use for switchable materials.

Furthermore, the THF in complex **10-La** was fully removed after drying it under high vacuum at 60 °C for several days, which produced the poorly soluble polymeric species $[La^{III}(\mu\text{-}\eta^2\text{:}\eta^2\text{-}BH_4)_2(\eta^3\text{-}BH_4)(\eta^9\text{-Cnt})]$ (**12-La**) in extremely low yield, as only a few single crystals were obtained from toluene (Scheme 10). The polymeric structure is best described as a trigonal-prismatic coordination polymer, in which each $La^{III}$ ion is coordinated by one Cnt ring ($\eta^9$), one terminal $BH_4$ ligand ($\eta^3$), and two bridging $BH_4$ ($\mu$-$\eta^2$:$\eta^2$) ligands. NMR spectroscopy showed a single peak for the Cnt both in the $^1$H ($\delta$ 7.44 ppm) and $^{13}$C NMR ($\delta$ 113.4 ppm) spectra and confirmed the presence of the $BH_4$ groups.

## Tris(cyclononatetraenyl) rare-earth complexes

In 2022, Nocton *et al.* reported the reactions between the potassium salt K(Cnt) and $LnI_3$ in toluene at room temperature, which led to the formation of a series of tris(Cnt) complexes **13-Ln** (Ln = Y, Gd, Tb, Dy, Ho, Er, and Tm) with the medium-sized to smaller lanthanides (Scheme 12).[45] A 3 : 1 ratio reaction is optimal, but 2 : 1 and 1 : 1 ratio reactions also gave the $[Ln^{III}(Cnt)_3]$ products in lower yields. The reaction time and yield varied with the ionic radii of the lanthanides: for Y, Gd, Tb and Dy, the reaction takes three to four days with moderate yields of 33–37%. For Ho and Er, the reaction required two to three weeks, and the isolated yield is 21% for **13-Ho** and 23% for **13-Er**. In contrast, for the smaller Tm, the reaction proceeded for six weeks and the obtained yield of **13-Tm** was only 15%. When $SmI_3(thf)_4$ or $YbI_3(thf)_3$ were employed in the reaction with K(Cnt), spontaneous reduction occurred and the bis(Cnt) complexes $[Ln^{II}(Cnt)_2]$ (**3-Ln**) were formed (Scheme 12). Attempts to use oxidizing agents (AgI or $FeCl_3$) to obtain the desired $[Ln^{III}(Cnt)_3]$ (Ln = Sm, Eu) were unsuccessful. Steric factors might partly explain this reduction, but the higher redox potential of $[Ln^{II}(Cnt)_2]$ compared to $[Ln^{II}(Cp^*)_2]$ might also be a reason that facilitates the reduction. Moreover, electronic contributions should also not be neglected, as the net valence of the Ln metal in $[Sm(Cp)_3]$ and $[Yb(Cp)_3]$ is not an integer but consists of multiconfigurational intermediate states.

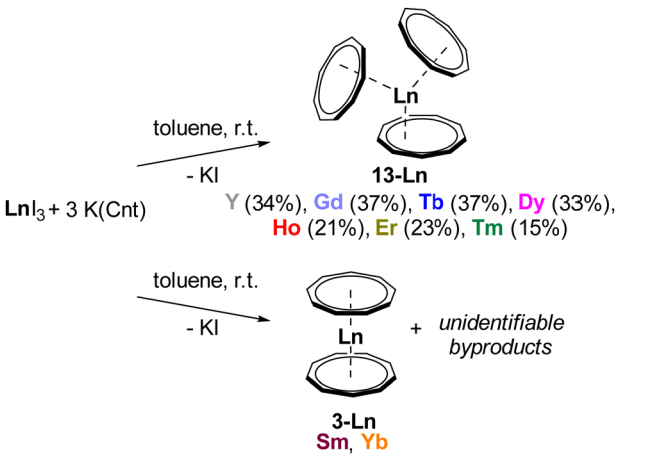


Scheme 12 Synthesis of the tris(Cnt) complexes **13-Ln** and reaction between K(Cnt) and $LnI_3$ (Ln = Sm, Yb), leading to $[Ln^{II}(Cnt)_2]$ (**3-Sm** and **3-Yb**).

 

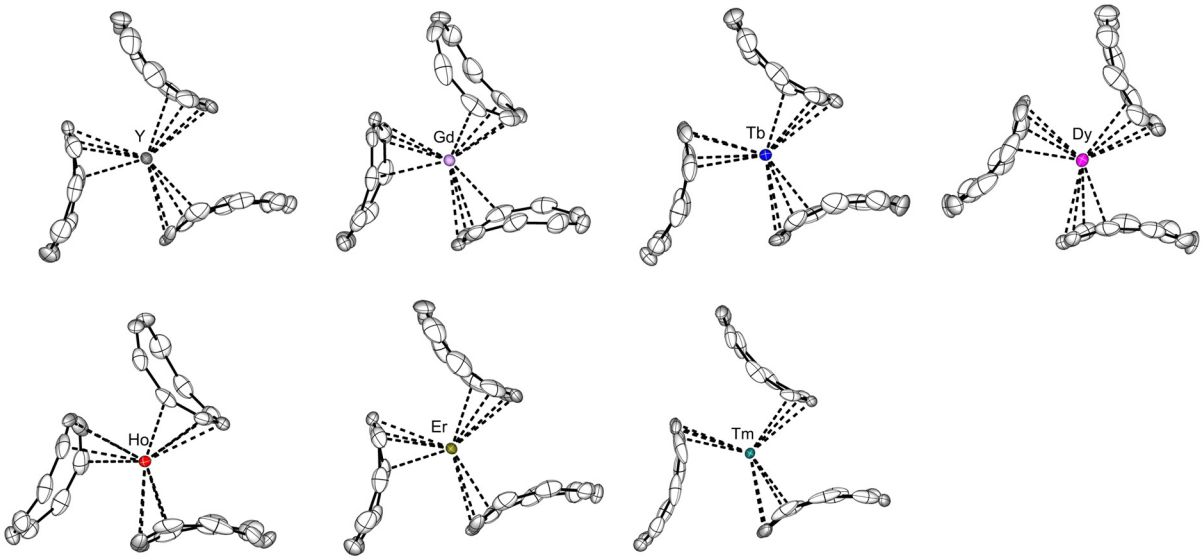


Fig. 10 Molecular structures of $[Ln^{III}(Cnt)_3]$ (**13-Ln**, Ln = Y, Gd, Tb, Dy, Er, Ho, Tm) in the solid state with thermal ellipsoids at 40% probability.†

SCXRD analysis revealed that all the complexes **13-Ln** (Y-Er) are isostructural (Fig. 10). Instead of the typical $\eta^9$-coordination modes in the bis(Cnt) sandwich type complexes **3-Ln**, all the Cnt ligands are consistently $\eta^4$-coordinating to the $Ln^{III}$ centres. Despite significant bending of the Cnt ligands around the $Ln^{III}$ ions, their aromaticity remains intact, without significant changes in C–C bond distances or C($sp^2$) hybridisation. There are interesting trends which nicely correlate with the ionic radii along the lanthanide series (Table 4): The shortest Ln–C bond was found to be 2.63(2) Å for the gadolinium complex **13-Gd** and 2.54(1) Å for the thulium complex **13-Tm**. A similar trend was observed for the average Ln–$C^4$ distance, reflecting the lanthanide contraction along the series. Overall, the average Ln–$C^9$ distance does not show any obvious trend and is rather similar for all seven compounds, suggesting a dynamic coordination behaviour of the Cnt ligand. An increase in $Ln^{III}$ size pushes the closest C atoms away but brings the farthest ones closer.

Due to the lability of the Cnt ligand in THF, $^1$H NMR spectra were recorded for all **13-Ln** complexes in toluene-$d_8$ to ensure their stability. For the Gd complex **13-Gd**, the $^1$H NMR spectrum remained silent. For the diamagnetic Y complex **13-Y**, only one singlet signal for the Cnt protons was found at $\delta$ 6.27 ppm. For all the other paramagnetic Ln species, this Cnt proton signal appeared as broad singlet at $\delta$ 295.5 ppm (**13-Tb**), $\delta$ 287.5 ppm (**13-Dy**), $\delta$ 273.0 ppm (**13-Ho**), $\delta$ 226.5 ppm (**13-Er**) and $\delta$ 264.3 ppm (**13-Tm**), showing a clear trend along the Ln series. The coordination environment is not temperature dependent, as the VT $^1$H NMR of **13-Y** showed little change from −80 °C to 80 °C. According to UV-vis spectroscopy, typical ligand-based π to π* transitions were detected for all complexes in the visible region, with **13-Er** and **13-Tm** exhibiting hypersensitive f–f transitions. An additional charge-transfer band was observed for **13-Tm**. Magnetic susceptibility measurements for all paramagnetic complexes **13-Ln** matched well with the nature of the trivalent $Ln^{III}$ ions. None of the tris(Cnt) complexes displayed single molecule magnet behaviour. Computational studies further interpreted the electronic structures and the magnetic behaviour, suggesting that the Cnt ligands in **13-Ln** provide a spherical crystal field.

## Summary and outlook

Compared to the classical smaller aromatic carbocyclic ligands, the 10π-electron cyclononatetraenyl (Cnt) monoanion has been part of the organolanthanide chemistry for less than ten years. Since its first coordination towards Ln in 2017, the chemistry of Cnt has expanded rapidly in the area of the lanthanides. Whilst classical homoleptic and heteroleptic sandwich-type complexes can be obtained using Cnt ligands, the large diameter and low charge density make the Cnt ligand more flexible and labile in

Table 4 Important metric parameters for **13-Ln**

| | 13-Y | 13-Gd | 13-Tb | 13-Dy | 13-Ho | 13-Er | 13-Tm |
|---|---|---|---|---|---|---|---|
| Ln–C (closest) | 2.58(1) | 2.63(2) | 2.61(2) | 2.58(3) | 2.59(2) | 2.56(2) | 2.54(1) |
| Ln–C (farthest) | 4.40(18) | 4.41(18) | 4.40(19) | 4.41(18) | 4.42(18) | 4.43(18) | 4.48(3) |
| Ln–$C^9$ (av.)[a] | 3.35(7) | 3.38(9) | 3.37(10) | 3.37(10) | 3.37(11) | 3.37(10) | 3.40(3) |
| Ln–$C^4$ (av.)[b] | 2.69(14) | 2.73(12) | 2.71(13) | 2.70(14) | 2.69(14) | 2.69(15) | 2.57(16) |

Distances are given in Å. [a] Average of the nine C atoms in the Cnt ring. [b] Average of the four closest C atoms in the Cnt ring.

coordination chemistry. For instance, the hapticity is often lower than $\eta^9$, or the Cnt ligand can be easily displaced from the metal centre using coordinating solvents. This feature initially seems disadvantageous but opens the door for applications as switchable materials (*e.g.*, luminophores, SMMs). The successful integration of the Cnt ligands with divalent and trivalent lanthanides open new avenues in lanthanide chemistry, the reported works clearly showcase that the Cnt ligand provides structures and reactivities which differ significantly from those of the classical Cp and Cot ligands in lanthanide chemistry. Currently, only the unsubstituted Cnt ligand has been utilised. One possible future direction is to introduce different substituents on the ring to enhance the solubility and modify the electronic and steric properties, similar as described for the well-known Cot ligand.

## Data availability

No primary research results, software or code have been included and no new data were generated or analysed as part of this review.

## Conflicts of interest

There are no conflicts to declare.

## Acknowledgements

The authors gratefully acknowledge support from the Deutsche Forschungsgemeinschaft (DFG, German Research Foundation) through the Collaborative Research Centre ''4f for Future'' (CRC 1573 project number 471424360, project C1).

## Notes and references

1 M. Faraday, *Philos. Trans. R. Soc.*, 1825, **115**, 440–466.
2 Z. Chen, C. S. Wannere, C. Corminboeuf, R. Puchta and P. V. R. Schleyer, *Chem. Rev.*, 2005, **105**, 3842–3888.
3 E. Hückel, *Z. Phys.*, 1931, **70**, 204–286.
4 T. J. Kealy and P. L. Pauson, *Nature*, 1951, **168**, 1039–1040.
5 G. Wilkinson, M. Rosenblum, M. C. Whiting and R. B. Woodward, *J. Am. Chem. Soc.*, 1952, **74**, 2125–2126.
6 G. Wilkinson and J. M. Birmingham, *J. Am. Chem. Soc.*, 1954, **76**, 6210.
7 A. Streitwieser and U. Mueller-Westerhoff, *J. Am. Chem. Soc.*, 1968, **90**, 7364.
8 F. Mares, K. Hodgson and A. Streitwieser, *J. Organomet. Chem.*, 1970, **24**, C68–C70.
9 J. G. Brennan, F. G. N. Cloke, A. A. Sameh and A. Zalkin, *J. Chem. Soc., Chem. Commun.*, 1987, 1668–1669.
10 J. P. Durrant, B. M. Day, J. Tang, A. Mansikkamäki and R. A. Layfield, *Angew. Chem., Int. Ed.*, 2022, **61**, e202200525.
11 B. M. Day, F.-S. Guo, S. R. Giblin, A. Sekiguchi, A. Mansikkamäki and R. A. Layfield, *Chem. Eur. J.*, 2018, **24**, 16779–16782.
12 L. Münzfeld, A. Hauser, P. Hädinger, F. Weigend and P. W. Roesky, *Angew. Chem., Int. Ed.*, 2021, **60**, 24493–24499.
13 L. Münzfeld, S. Gillhuber, A. Hauser, S. Lebedkin, P. Hädinger, N. D. Knöfel, C. Zovko, M. T. Gamer, F. Weigend, M. M. Kappes and P. W. Roesky, *Nature*, 2023, **620**, 92–96.
14 F. T. Edelmann, *New J. Chem.*, 2011, **35**, 517–528.
15 K. L. M. Harriman, J. J. Le Roy, L. Ungur, R. J. Holmberg, I. Korobkov and M. Murugesu, *Chem. Sci.*, 2017, **8**, 231–240.
16 A. Hauser, L. Münzfeld, S. Schlittenhardt, C. Uhlmann, L. Leyen, E. Moreno-Pineda, M. Ruben and P. W. Roesky, *J. Am. Chem. Soc.*, 2024, **146**, 13760–13769.
17 T. Arliguie, M. Lance, M. Nierlich and M. Ephritikhine, *J. Chem. Soc., Dalton Trans.*, 1997, 2501–2504.
18 K. Kawasaki, R. Sugiyama, T. Tsuji, T. Iwasa, H. Tsunoyama, Y. Mizuhata, N. Tokitoh and A. Nakajima, *Chem. Commun.*, 2017, **53**, 6557–6560.
19 T. J. Katz and P. J. Garratt, *J. Am. Chem. Soc.*, 1963, **85**, 2852–2853.
20 E. A. Lalancette and R. E. Benson, *J. Am. Chem. Soc.*, 1963, **85**, 2853.
21 P. Radlick and G. Alford, *J. Am. Chem. Soc.*, 1969, **91**, 6529–6530.
22 G. Boche and F. Heidenhain, *J. Organomet. Chem.*, 1976, **121**, C49–C51.
23 H. T. Verkouw, M. E. E. Veldman, C. J. Groenenboom, H. O. Van Oven and H. J. De Leifde Meijer, *J. Organomet. Chem.*, 1975, **102**, 49–56.
24 A. Westerhof and H. J. De Liefde Meijer, *J. Organomet. Chem.*, 1978, **149**, 321–325.
25 T. Murahashi, R. Inoue, K. Usui and S. Ogoshi, *J. Am. Chem. Soc.*, 2009, **131**, 9888–9889.
26 M. Xémard, S. Zimmer, M. Cordier, V. Goudy, L. Ricard, C. Clavaguéra and G. Nocton, *J. Am. Chem. Soc.*, 2018, **140**, 14433–14439.
27 L. Münzfeld, C. Schoo, S. Bestgen, E. Moreno-Pineda, R. Köppe, M. Ruben and P. W. Roesky, *Nat. Commun.*, 2019, **10**, 3135.
28 G. Boche and A. Bieberbach, *Chem. Ber.*, 1978, **111**, 2850–2858.
29 F. Mares, K. O. Hodgson and A. Streitwieser, *J. Organomet. Chem.*, 1971, **28**, C24–C26.
30 M. D. Walter, G. Wolmershäuser and H. Sitzmann, *J. Am. Chem. Soc.*, 2005, **127**, 17494–17503.
31 S. Harder, D. Naglav, C. Ruspic, C. Wickleder, M. Adlung, W. Hermes, M. Eul, R. Pöttgen, D. B. Rego, F. Poineau, K. R. Czerwinski, R. H. Herber and I. Nowik, *Chem. Eur. J.*, 2013, **19**, 12272–12280.
32 R. P. Kelly, T. D. M. Bell, R. P. Cox, D. P. Daniels, G. B. Deacon, F. Jaroschik, P. C. Junk, X. F. Le Goff, G. Lemercier, A. Martinez, J. Wang and D. Werner, *Organometallics*, 2015, **34**, 5624–5636.
33 T. Tsuji, S. Fukazawa, R. Sugiyama, K. Kawasaki, T. Iwasa, H. Tsunoyama, N. Tokitoh and A. Nakajima, *Chem. Phys. Lett.*, 2014, **595–596**, 144–150.
34 H. Ramanantoanina, L. Merzoud, J. T. Muya, H. Chermette and C. Daul, *J. Phys. Chem. A*, 2020, **124**, 152–164.
35 T. Vitova, H. Ramanantoanina, B. Schacherl, L. Münzfeld, A. Hauser, R. S. K. Ekanayake, C. Y. Reitz, T. Prüßmann, T. S. Neill, J. Göttlicher, R. Steininger, V. A. Saveleva, M. W. Haverkort and P. W. Roesky, *J. Am. Chem. Soc.*, 2024, **146**, 20577–20583.
36 K. O. Hodgson, F. Mares, D. F. Starks and A. Streitwieser, *J. Am. Chem. Soc.*, 1973, **95**, 8650–8658.
37 K. Mashima, Y. Nakayama, A. Nakamura, N. Kanehisa, Y. Kai and H. Takaya, *J. Organomet. Chem.*, 1994, **473**, 85–91.
38 M. Tricoire, L. Münzfeld, J. Moutet, N. Mahieu, L. La Droitte, E. Moreno-Pineda, F. Gendron, J. D. Hilgar, J. D. Rinehart, M. Ruben, B. Le Guennic, O. Cador, P. W. Roesky and G. Nocton, *Chem. – Eur. J.*, 2021, **27**, 13558–13567.
39 G. Boche, D. Martens and W. Danzer, *Angew. Chem., Int. Ed. Engl.*, 1969, **8**, 984.
40 G. Boche, H. Weber, D. Martens and A. Bieberbach, *Chem. Ber.*, 1978, **111**, 2480–2496.
41 L. Münzfeld, M. Dahlen, A. Hauser, N. Mahieu, S. K. Kuppusamy, J. Moutet, M. Tricoire, R. Köppe, L. La Droitte, O. Cador, B. Le Guennic, G. Nocton, E. Moreno-Pineda, M. Ruben and P. W. Roesky, *Angew. Chem., Int. Ed.*, 2023, **62**, e202218107.
42 L. Pedussaut, N. Mahieu, C. Chartier, T. Rajeshkumar, I. Douair, N. Casaretto, L. Maron, G. Danoun and G. Nocton, *Chem. Sci.*, 2024, **15**, 19273–19282.
43 L. Münzfeld, A. Hauser, M. T. Gamer and P. W. Roesky, *Chem. Commun.*, 2023, **59**, 9070–9073.
44 L. Münzfeld, X. Sun, S. Schlittenhardt, C. Schoo, A. Hauser, S. Gillhuber, F. Weigend, M. Ruben and P. W. Roesky, *Chem. Sci.*, 2022, **13**, 945–954.
45 O. Stetsiuk, L. La Droitte, V. Goudy, B. Le Guennic, O. Cador and G. Nocton, *Organometallics*, 2022, **41**, 133–140.

 